JOURNAL OF CATALYSIS 62, 264–274 (1980)

Reactions of Methanol on W(100) and W(100)–(5 × 1)C Surfaces

E. I. Ko, J. B. Benziger, and R. J. Madix

Department of Chemical Engineering, Standford University, Stanford, California 94305

Received March 28, 1979; revised August 24, 1979

The decomposition of methanol-OD was studied on W(100) and W(100)–(5 × 1)C surfaces by temperature-programmed reaction spectroscopy. Initial adsorption of methanol-OD on the clean W(100) surface resulted in the complete dissociation of the molecule into hydrogen, carbon, and oxygen (β-CO). Methane, methanol-OH, and formaldehyde were observed as additional products after the CO(β) states had been saturated. The W(100)–(5 × 1)C surface produced the same products with the addition of carbon dioxide, water, and methyl formate. Moreover, the carbide surface enhanced the selectivity for hydrocarbon formation by an order of magnitude compared to the clean surface due to the suppression of the dissociation of methanol to β-CO and H_2 on the carbon chemilayer. The reaction mechanism was explained in terms of three intermediates: methoxy, formate, and a surface complex comprised of methoxy radicals and trapped hydrogen atoms. The "trapped" hydrogen atoms were apparently stabilized by the methoxy intermediates.

1. INTRODUCTION

A wide variety of industrial processes use metal catalysts. Common examples are transition metals (Pt, Ni) supported on nonmetallic substrates (Al_2O_3, Si_2O_3). Due to the scarcity and the high cost of noble metals, there is a strong incentive for the development of novel catalytic materials. One approach is to modify the chemical properties of originally unattractive metals. This may be achieved by alloying the metal with another metal or with other elements such as carbon and nitrogen. In recent years there have been many studies of the catalytic properties of carbides, with special emphasis on the modification of the catalytic properties of metals due to carbon. Sinfelt and Yates observed that the formation of molybdenum carbide enhanced the activity for ethane hydrogenolysis over supported molybdenum carbide catalysts (*1*). Levy and Boudart found that WC exhibited platinum-like behavior for several test reactions (*2*). Ross and Stonehart, in search of a substrate for Pt as an electrode material, reported that the electrocatalytic activity of tungsten carbide was sensitive to surface composition (*3–5*). Under UHV conditions, McCarty and Madix showed that surface carbon significantly altered the activity and selectivity of a Ni(110) single crystal for the decomposition of formic acid, providing surface reactivity characteristics of copper (*6*). Further studies on Ni(100) and Ni(100)–p(2 × 2)C support this conclusion (*7*). In recent work with a W(100) single crystal it was shown that the chemisorption behavior of hydrogen and carbon monoxide on tungsten was drastically affected by carburization (*8*). In particular, the W(100)–(5 × 1)C chemilayer surface was incapable of dissociatively adsorbing CO, and hydrogen adsorption was reduced at room temperature by a factor of 50 with respect to W(100). The pronounced effects of surface carbon on these simple molecules prompted us to study more complex reaction systems. The surface reactions following formaldehyde, methanol, and methyl formate adsorption have been investigated on the W(100) and the W(100)–(5 × 1)C surfaces. In all cases the product distributions were markedly different on the two surfaces. The results for methanol are reported here. The results for the other two reactions will be presented subsequently (*9, 10*).

0021-9517/80/040264-11$02.00/0

2. EXPERIMENTAL

The flash desorption experiments were performed in the stainless-steel ultrahigh vacuum system previously described (*8*). The system was equipped with four-grid LEED optics, a cylindrical mirror analyzer with an integral electron gun, and a quadrupole mass spectrometer. The tungsten crystal was heated by radiation from a tungsten filament located 3 mm behind the crystal for flash desorption studies or by electron bombardment for cleaning. A heating rate of 20 K sec^{-1} was used throughout. Methanol vapor was introduced to the sample through a 22-gauge stainless-steel needle directed toward the crystal face. The crystal was turned to face the mass spectrometer during the flash to enhance the signal-to-noise ratio and to minimize the effect of differing pumping speeds on the detection sensitivity for various products. The reaction products were monitored by the major mass cracking fractions and corrected for overlapping signals. The formation of $HCOOCH_3$, CH_3OH, CH_3OD, H_2CO, and CH_4 was monitored by m/e = 60, 31, 33, 30, and 16, respectively. The choice of m/e = 60, which is a sizable cracking fragment of methyl formate but not of glycoaldehyde (*11*), enabled a distinction between these two isomers.

The W(100) surface was cleaned by heating in 5 × 10^{-6} Torr oxygen for 2–3 hr at 1500 K followed by a brief flash to 2500 K in vacuum. The clean (100) surface structure was verified by LEED and AES. Surface contamination due to carbon and oxygen from the reaction was readily removed by flashing the sample to 2500 K in vacuum. Preparation of the W(100)–(5 × 1)C surface has been described in detail elsewhere (*8*). Surface carbon was deposited by cracking ethylene at 1500 K until a distinct (5 × 1)C LEED pattern was obtained. The carbide surface was easily reproduced and suffered no degradation subsequent to 20–30 adsorption–desorption cycles.

Deuterated methanol, CH_3OD (99 atm%), was obtained from ICN Life Science and purified by prolonged pumping at 228 K (chlorobenzene solid–liquid bath) until a constant vapor pressure of 800 μ was achieved. The sample line was then pumped down to 200 μ for better control over the exposure.

3. RESULTS

3.1. Methanol Decomposition on the Clean Surface

The product distribution subsequent to saturation exposure of CH_3OD at room temperature on the W(100) surface is shown in Fig. 1. The product peaks were corrected for relative mass spectrometer sensitivities following the procedure outlined in the Appendix. Deuterated metha-

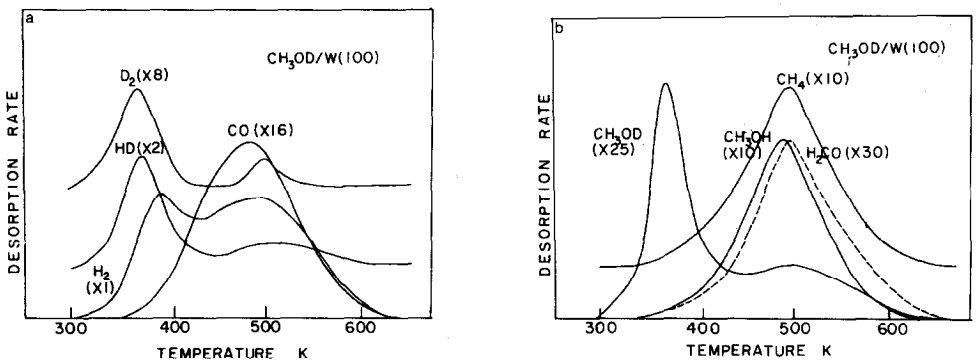

FIG. 1. (a, b) Product distribution subsequent to saturation exposure of CH_3OD at room temperature on W(100).

nol, CH_3OD, was used in this study so that the hydroxyl hydrogen could be distinguished from the methyl hydrogen. Low exposures of the initially clean W(100) surface to CH_3OD led to complete dissociation of the parent molecule into surface hydrogen atoms and CO; the latter was further dissociated into surface carbon and oxygen, populating the CO(β) states. CO(β) desorbed from W(100) at temperatures higher than those achievable in the flash desorption experiments and consequently is not shown among the product peaks; surface carbon and oxygen were therefore monitored by AES. Hydrogen evolution was observed from 300 to 600 K with two apparent desorption rate maxima at 385 and 500 K. The HD and D_2 desorption spectra showed a similar two-peak structure although the relative areas of the two peaks differed. At higher exposures of CH_3OD additional products including methane, methanol, and formaldehyde were observed. Unreacted CH_3OD desorbed from the surface at 370 K. The CH_3OD shoulder at 500 K was the result of a decomposition step to be discussed below. CH_3OH was observed as a product desorbing at around 490 K even though CH_3OD was initially adsorbed. This suggested that methoxy was a stable surface intermediate which decomposed to yield CH_3OH, H_2CO, H_2, and CO near 500 K. Methoxy has previously been found to be the abundant surface intermediate for the decomposition of methanol on Cu (*12*) and Ag (*13*). However, the observation of methane formation in this study was unique. Quantitative measurements of the gaseous products desorbing at 500 K gave an overall atomic stoichiometry of $CH_{4.5}O_{0.8}$.

The buildup of carbon and oxygen detected by AES after the desorption of the reaction products was due to the filling of the CO(β) states as noted above. It was possible to desorb all of the CO(β) by heating the sample with electron bombardment to 1500 K. An Auger spectrum taken immediately after heating to 1500 K revealed that the reactions of CH_3OD also yielded additional adsorbed oxygen as a reaction product. Moreover, the amount of adsorbed oxygen was identical to the amount of methane formed within experimental uncertainty. With this residual oxygen taken into account, the stoichiometry of the adsorbed phase above 400 K excluding CO(β) states was $CH_{4.5}O$. The product yields corresponding to saturation exposure of CH_3OD are summarized in Table 1. The absolute coverages were calculated using an empirical approach outlined in the Appendix. The amount of adsorbed oxygen was determined by AES using the CO(β) saturated W(100) surface as a calibration standard (*8*, *14*). The CO(γ) and CO(β) states combined accounted for 84% of the total products, whereas the yields for H_2CO, CH_3OH, and CH_4 were each an order of magnitude less. The hydrocarbon selectivity for the reaction, defined as the total molecular yield of hydrocarbons divided by the total CO yield, was 0.2 at saturation. No other products other than those listed in Table 1 were detected following the decomposition of CH_3OD on the initially clean W(100) surface.

TABLE 1

Product Yields for CH_3OD Decomposition (Saturation Exposure)

Product	Molecules/cm²	
	W(100)	W(100)-(5 × 1)C
H_2, HD, D_2	3.6×10^{14}[a]	7.3×10^{13}
CO(γ)	2.6×10^{13}	3.7×10^{13}
CO(β)	4.3×10^{14}	—
CH_4	3.7×10^{13}	3.4×10^{13}
H_2CO	1.2×10^{13}	0.8×10^{13}
CH_3OH	3.7×10^{13}	4.0×10^{13}
CH_3OD	1.5×10^{13}	1.5×10^{14}
$HCOOCH_3$	—	0.2×10^{13}
CO_2	—	0.1×10^{13}
H_2O	—	0.1×10^{13}
O(a)	3×10^{13}	3×10^{13}

[a] Hydrogen displaced during adsorption was not included.

3.2. *Methanol Decomposition on the Carbide Surface*

The surface reactions subsequent to adsorption of CH_3OD on the W(100)–(5 × 1)C surface at 250 K produced hydrogen, carbon monoxide, carbon dioxide, water, methane, formaldehyde, methanol, methanol-OD, and methyl formate (Fig. 2). The carbide surface did not dissociate CO, so the CO desorption spectrum reflected the *total* amount of CO product. Coverage variation studies with CH_3OD showed that the CO spectrum consisted of first-order peaks at 397 and 435 K; a third peak was observed with its maximum shifting from 525 to 470 K with increasing coverage. The CO peak at 397 K developed at the lowest coverages, followed by the 470 K peak and then the 435 K peak as the coverage was increased (Fig. 3). The CO_2 peak, which desorbed by a first-order process at 555 K, originated from a formate intermediate, as the coincident evolution of H_2 and CO_2 was observed at the same temperature for the decomposition of HCOOH on W(100)–(5 × 1)C (*15*). Unreacted CH_3OD desorbed at 390 K with a shoulder at 300 K which was evident only at high exposures. CH_3OH, CO, and H_2 desorbed at 435 K. The coincident evolution of hydrogen, methanol, methane, formaldehyde, and CO was observed at 470 K. The sum of the various products at 470 K, excluding the residual adsorbed oxygen, gave an overall stoichiometry of $CH_{4.5}O_{0.8}$, as in the case of the clean surface. The shift of the peak temperature of these products with increasing coverage was indicative of either a second-order desorption process or a coverage-dependent activation energy. An isotherm–isostere plot (*16*) showed that the desorption order changed from 1.8 to 1.0 as the coverage was decreased. Since the apparent desorption order should be constant for a true second-order desorption process, the results indicated a coverage-dependent activation energy, probably arising from lateral interactions on the surface. The product yields for the W(100)–(5 × 1)C surface are summarized in Table 1. Of the CH_3OD that reacted, nearly equal amounts of CO, CH_3OH, and CH_4 were produced. The selectivity for hydrocarbon formation was 2.3 which represented an order of magnitude enhancement over that observed on the clean surface. In addition, the carbide surface produced methyl formate, which was not found on the clean surface. The decomposition of CH_3OD also resulted in a slight oxygen buildup on the W(100)–(5 × 1)C surface as shown in Table 1.

4. DISCUSSION

The results of the preceding section led to the following deductions concerning the surface reaction of CH_3OD on the W(100) and the W(100)–(5 × 1)C surfaces:

(i) Initial adsorption on the clean W(100) surface led to immediate dissociation of the parent molecule into hydrogen, carbon, and

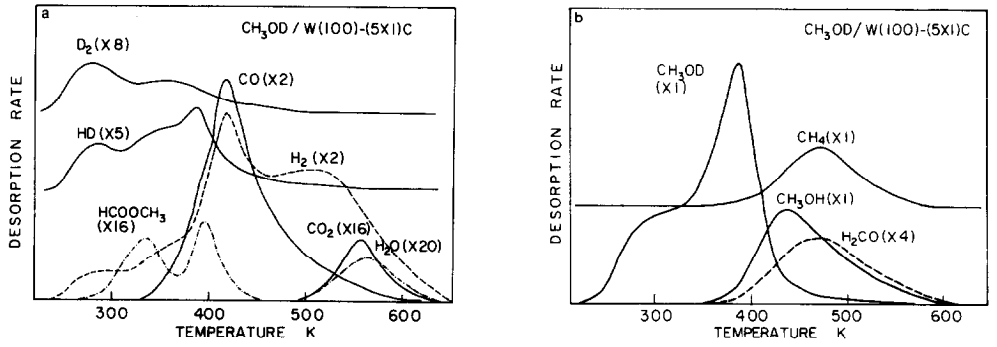

FIG. 2. (a, b) Product distribution subsequent to saturation exposure of CH_3OD at 250 K on W(100)–(5 × 1)C.

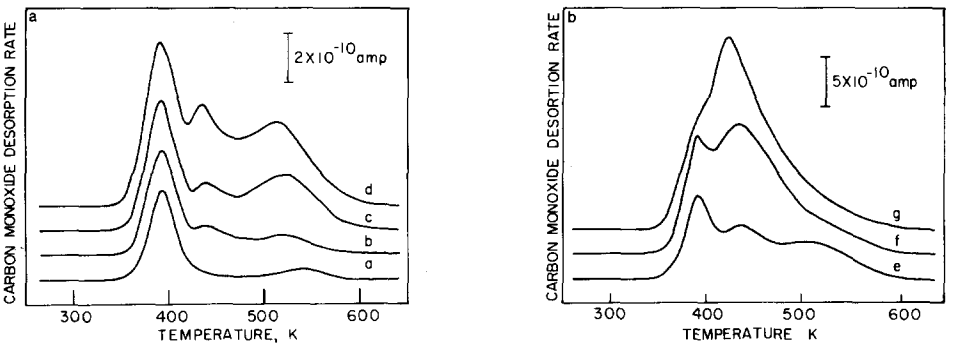

FIG. 3. Carbon monoxide desorption following CH_3OD adsorption at 250 K on W(100)-(5 × 1)C as a function of exposure: (a) 0.02L; (b) 0.04L; (c) 0.1L; (d) 0.2L; (e) 0.4L; (f) 0.8L; (g) 2L.

oxygen. The formation of hydrocarbons (methane, methanol, formaldehyde) was observed only after more than 80% of the CO(β) states had been populated.

(ii) The reactivity of the tungsten surface was partially passivated by surface carbon in the form of a carbide chemilayer. On the carbide surface molecular CH_3OD did not completely dissociate. Under these conditions the formation of hydrocarbons were favored, resulting in a significant shift in the reaction selectivity, as illustrated in Table 1.

(iii) The most abundant surface intermediate observed was of stoichiometric composition $CH_{4.5}O$. When heated, this intermediate produced methanol, methane, formaldehyde, surface oxygen, H_2, and CO. The composition of the intermediate represented a stoichiometric excess of hydrogen with respect to the parent molecule. The overall stoichiometry of CH_3OD was recovered in the products desorbing from the (5 × 1)C surface but not from the clean surface due to the displacement of hydrogen from the surface during exposure, similar to that observed with H_2, CO coadsorption.

Egelhoff *et al.* (*17*) concluded from UPS that low exposure of W(100) to methanol at room temperature generated an adsorbed layer of hydrogen atoms and CO. At higher exposures adsorption without complete decomposition occurred, and UPS showd evidence for a molecular surface complex. This complex decomposed upon heating to 700 K, increasing the CO coverage in the residual layer. In this work we also observed that initial adsorption of CH_3OD on the clean W(100) surface resulted in the complete dissociation of the alcohol into hydrogen and CO(β). Higher exposures led to the formation of stable intermediates as the surface reactivity became passivated by CO(β). The coincident evolution of H_2CO, CH_3OH, H_2, and CO from methanol was characteristic of the decomposition of the methoxy intermediate found for several other systems (*12, 13, 18, 19*). The formation of methane as a major hydrocarbon product, on the other hand, was not observed. In accordance with the stoichiometric composition of $CH_{4.5}O$, it appeared that the products near 500 K originated from a surface complex comprised of methoxy radicals and trapped hydrogen atoms. Surface hydrogen atoms, produced either from the cracking of the parent molecule or the decomposition of methoxys at 435 K, were apparently trapped, or stabilized, by methoxy intermediates. Both hydrogen and alkoxides are known to bridge-bond to metal atoms and alkoxide hydrides are commonly known in transition metal complexes (*20, 21*). To ascertain the necessity of surface hydrogen atoms in forming the complex, the decomposition of CH_3OD was studied on a W(100) surface presaturated with CO(β) (*22*). The coincident evolution of H_2, CO, H_2CO, and CH_3OH characteris-

tic of the decomposition of methoxy was observed at 416 K but *no* methane formation was noted. Correspondingly the overall stoichiometry of these products showed no hydrogen surplus. Furthermore, the CO(β) saturated surface was less reactive than the clean W(100) surface, since a large portion of adsorbed CH_3OD desorbed unreacted. Intact methanol molecules were therefore the most abundant surface species on the CO(β) saturated surface. This behavior was consistent with the findings of Egelhoff *et al.* (*17*) who observed from thier photoemission spectra different molecular complexes on the clean and the CO(β) saturated surface; on the latter surface the spectrum was similar to that of gaseous methanol. It should be noted that on the initially clean W(100) surface the complex, once formed, did not decompose until 500 K. This was well above the desorption limited peak temperatures for hydrogen, as the binding energy of hydrogen was reduced on a CO(β) saturated surface (*23, 24*). In fact, at high methanol exposures the displacement of hydrogen atoms from the surface took place, reflected by the hydrogen deficiency in the overall stoichiometric balance.

The results obtained in this work are also consistent with the observations reported by Gasser *et al.* (*25*) who studied methanol decomposition on a tungsten filament. They found that carbon monoxide and hydrogen were the overwhelming products over the temperature range 550 to 2000 K on a clean filament. However, under steady-state conditions methane and formaldehyde were observed as additional products for filament temperatures between 600 and 1400 K; at temperatures above 1500 K the reaction produced only CO and H_2. The results presented here show that the change in selectivity could be accounted for by the formation of adsorbed oxygen and carbon on the surface at the lower temperatures rather than surface oxygen alone as they suggested.

The passivation of the tungsten surface to favor hydrocarbon formation was also achieved by carburization. In addition, the presence of surface carbon reduced the total reactivity (measured as the percentage of methanol molecules reacted subsequent to adsorption). The W(100)–(5 × 1)C surface dissociated only about half of the adsorbed methanol, compared to over 90% conversion for the clean surface (Table 2). As in the case for the clean surface, the stoichiometry of the products evolved at 470 K showed an adsorbed hydrogen atom surplus compared to CH_3O(a). The overall stoichiometry of the parent molecule, on the other hand, was correctly recovered when all reaction products were included over the entire temperature range. The data suggested that some of the methoxy decomposed at 400 K liberating hydrogen, carbon monoxide, and formaldehyde. CO desorbed immediately into the gas phase, as it was formed above the desorption temperature for α-CO/CO on the W(100)–(5 × 1)C surface (*8*). Formaldehyde underwent recombination with methoxide and led to the formation of methyl formate which desorbed at 400 K in a reaction limited step (*10*). As discussed earlier for the clean surface, some of the hydrogen atoms released were trapped, or stabilized, by neighboring methoxides resulting in the formation of a new surface complex with a stoichiometric excess of hydrogen as observed. The complex decomposed at 470 K giving rise to H_2, CO, H_2CO, CH_3OH, and CH_4. On the carbide surface hydrogen

TABLE 2

Activity for CH_3OD Decomposition

	Molecules/cm²	
	W(100)	W(100)–(5 × 1)C
CH_3OD adsorbed (based on carbon balance)	5.4×10^{14}	2.7×10^{14}
CH_3OD desorbed	1.5×10^{13}	1.5×10^{14}
Percentage reacted	97.3	44.4

atoms released from either the initial dehydrogenation of the parent molecule or the decomposition of methoxy at 400 K could be complexed. No methane was formed from the decomposition of isolated methoxys, which were responsible for the products at 400 and 435 K. The formation of methyl formate on the W(100)–(5 × 1)C surface was observed only at high surface coverages when the surface concentration of reactants was high, presumably giving a higher probability for two methoxys to be in close proximity.

The surface complex, $CH_{4.5}O$, exhibited lateral interactions on the carbide surface between nearest neighbors as manifested experimentally by the decrease of peak temperature with increasing coverage for all products desorbing at 470 K. The isotherm–isostere plots showed that the apparent reaction order changed from 1.8 to 1.0 for isothermal rates at 454 and 514 K, respectively. For a constant pre-exponential factor of 10^{13} sec^{-1} the corresponding change in activation energy was about 3 kcal/mole. No evidence for lateral interactions was observed for the clean surface, however, despite the fact that comparable surface concentrations of the intermediate were formed. The clean surface was different from the carburized surface in two respects. First, the clean surface was saturated with CO(β) states from the initial adsorption of CH_3OD. Second, the atomic structure of the clean surface possessed square symmetry in contrast to the hexagonal structure of the carbide surface (*8*). It was speculated that the surface intermediates on the clean surface were further separated and were distributed in a way unfavorable for lateral interactions. The spatial separation of surface intermediates could also account for the lack of methyl formate formation on this initially clean W(100) surface.

5. SUMMARY

The reactions of methanol subsequent to adsorption on well-defined surfaces of W(100) and W(100)–(5 × 1)C were as follows:

(*i*) *W(100)*

Initial adsorption on the clean surface

$$CH_3OD(g) \rightarrow C(a) + O(a) + 3H(a) + D(a)$$

At higher exposures

$$CH_3OD(g) \rightarrow CH_3O(a) + D(a)$$
$$CH_3OD(g) \rightarrow CH_3OD(a)$$

With increasing temperature

$$CH_3OD(a) \rightarrow CH_3OD(g)$$
$$H(a) + D(a) \rightarrow H_2(g) + HD(g) + D_2(g)$$

Some of the hydrogen atoms did not desorb and were stabilized by surface methoxys, leading to the formation of a surface complex denoted as Y. As the exact nature of the complex is unknown, the reaction step below does not represent an elementary step. Some of the methoxys decomposed into CO and hydrogen atoms. The hydrogen atoms took part in forming the complex and CO was dissociated and saturated the CO(β) states.

$$CH_3O(a) \rightarrow 3H(a) + C(a) + O(a)$$
$$CH_3O(a) + H(a) + D(a) \rightarrow Y(a)$$

The complex remained stable until 500 K, at which point it decomposed to yield methane, methanol, formaldehyde, hydrogen, carbon monoxide, and adsorbed oxygen.

$$Y(a) \rightarrow CH_4(g) + CH_3D(g) + CH_3OH(g) + CH_3OD(g) + H_2CO(g) + H(a) + D(a) + O(a)$$
$$H(a) + D(a) \rightarrow HD(g) + D_2(g)$$

(ii) W(100)-(5 × 1)C

The mechanism was similar to that on the clean surface except that CO(β) no longer played a role. Upon adsorption,

$$CH_3OD(g) \rightarrow CH_3OD(a)$$
$$CH_3OD(g) \rightarrow CH_3O(a) + D(a)$$

With increasing temperature

$$CH_3O(a) \rightarrow H_2CO(a) + H(a)$$
$$CH_3O(a) + H_2CO(a) \rightarrow HCOOCH_3(a) + H(a)$$
$$HCOOCH_3(a) \rightarrow HCOOCH_3(g)$$
$$CH_3OD(a) \rightarrow CH_3OD(g)$$
$$H(a) + D(a) \rightarrow H_2(g) + HD(g) + D_2(g)$$

As on the clean surface, some of the hydrogen atoms were trapped into complex Y. At around 400 K the decomposition of methoxy produced methyl formate, CO, and surface hydrogen atoms which then took part in the complex formation.

$$CH_3O(a) \rightarrow 3H(a) + CO(g)$$
$$CH_3O(a) \rightarrow H_2CO(a) + H(a)$$
$$H_2CO(a) + CH_3O(a) \rightarrow HCOOCH_3(g)$$
$$CH_3O(a) + H(a) + D(a) \rightarrow Y(a)$$

The complex decomposed at 470 K, giving rise to products analogous to those on the clean surface.

$$Y(a) \rightarrow CH_4(g) + CH_3D(g) + CH_3OH(g) + CH_3OD(g) + H_2CO(g) + H(a) + D(a) + O(a)$$
$$H(a) + D(a) \rightarrow H_2(g) + HD(g) + D_2(g)$$

Oxidation of formaldehyde led to the formation of formate which decomposed at 555 K,

$$HCOO(a) \rightarrow 2H(a) + CO_2(g)$$
$$H(a) + H(a) \rightarrow H_2(g)$$
$$2H(a) + O(a) \rightarrow H_2O(g)$$

At higher exposures the following reaction sequence took place at 435 K,

$$CH_3O(a) \rightarrow 3H(a) + CO(g)$$
$$CH_3O(a) + H(a) \rightarrow CH_3OH(g)$$
$$H(a) + H(a) \rightarrow H_2(g)$$

6. CONCLUSION

It has been shown that the selectivity for the surface reaction of methanol on W(100) was very sensitive to the composition of the surface. For the clean surface hydrogen

and carbon monoxide were the predominant products. Passivation of the tungsten surface either by saturation of the CO(β) states or by carburization resulted in the enhancement of the yields of hydrocarbons. In addition the formation of methyl formate was observed on the carbide surface. The formation of methane, methanol, and formaldehyde was ascribed to the decomposition of a stable intermediate composed of methoxide intermediates and stabilized surface hydrogen atoms. The results further illustrate the applicability of UHV techniques to the study of complex reacting systems on well-characterized single crystals.

APPENDIX

The technique of Temperature-Programmed Reaction Spectroscopy (TRPS) requires a quantitative analysis of mass spectral data. The ionization and detection processes of a mass spectrometer are complex and prohibit a theoretical approach to the deconvolution of such data. In order to extract quantitative information about product yields for multiple desorbing products, an empirical approach has been developed which accounts for differences in ionization efficiencies, mass spectrometer gain, mass fraction transmission, and the cracking of the parent molecule. This technique yielded results that were consistent for several reactants (*9, 10*). (The product spectra for adsorbed methanol will be used to exemplify this technique.)

In order to identify a gas from mass spectral data, the fragmentation pattern must be known. These were obtained by scanning the mass range of interest while admitting the desired gas into the vacuum system; Table A-1 summarizes the major mass cracking fractions for the species formed from methanol on W(100)–(5 × 1)C. Comparing fragmentation patterns we chose to monitor those which allow individual products to be identified with the greatest convenience. Two criteria were employed in the choice of the cracking fraction to be monitored; first it was a major fragmentation product which could be easily distinguished from the background signal and, second, it was identified as a fragment which originated from as few species as possible. In the case of a mass fragment resulting from multiple species other mass fragments were checked for consistency.

After the appropriate mass fragments were selected, a series of thermal desorption spectra were obtained for a fixed coverage and heating rate. For the case of methanol on W(100)–(5 × 1)C the thermal desorption spectra employed were methyl formate (m/e = 60), methanol (m/e = 32, 31), methanol-OD (m/e = 33), formaldehyde (m/e = 30), carbon dioxide (m/e = 44), carbon monoxide (m/e = 28), water (m/e = 18), and hydrogen (m/e = 2). The raw data were then corrected to reflect desorption spectra of single species. In the example at hand, the formaldehyde spec-

TABLE A-1

Fragmentation Patterns for Products

Species	60	44	33	32	31	30	29	28	18	16	15	14
$HCOOCH_3$	30	—	—	40	100	11	68	19	—	—	30	—
CH_3OD	—	—	79	100	3	9	18	—	—	—	10	—
CH_3OH	—	—	—	72	100	3	42	9	—	—	—	—
CH_4	—	—	—	—	—	—	—	—	—	100	86	17
CO	—	—	—	—	—	—	—	100	—	2	—	—
H_2CO	—	—	—	—	—	85	100	40	—	—	—	—
CO_2	—	100	—	—	—	—	—	20	—	20	—	—
H_2O	—	—	—	—	—	—	—	—	100	—	—	—

trum was corrected for the contribution due to methanol-OD by subtracting the m/e = 30 methanol-OD desorption spectrum from the total m/e = 30 desorption spectrum. As shown in Fig. A-1 the two low temperature m/e = 30 peaks were accounted for entirely by the cracking of CH_3OD, leaving the 470 K peak as the only formaldehyde product peak. The 470 K peak was further corrected for the contribution due to CH_3OH at the same temperature. Other similar corrections required were: m/e = 16 due to CO was subtracted from the total m/e = 16 to obtain the methane spectrum, and m/e = 28 due to CO_2, H_2CO, and CH_3OH was subtracted from the total m/e = 28 to obtain CO spectrum.

The mass fragment desorption spectra were then corrected to reflect rates of reaction, and to allow relative product yields to be obtained. The method employed was similar to that suggested by UTI (*26*) to correct for relative differences in ionization efficiency (I_x), quadrupole transmission (T_m), electron multiplier gain (G_m), and mass fragment yield (F_m) as given in Table A-1.

Ionization efficiency is primarily dependent on the number of electrons per molecule. A reasonable correlation for the total ionization efficiency of a molecule relative to CO is given by

$$I_x = 0.6\ \{\text{number of electrons}/14\} + 0.4$$

The gain of the electron multiplier is a function of ion mass, such that relative to CO it can be approximated as

$$G_M = (28/MW)^{1/2}$$

Transmission of an ion through the quadrupole filter is also a function of ion mass such that for the spectrometer used, UTI has determined that the transmission is approximately

$$T_m = \begin{cases} 10^{(30-MW)/155} & MW > 30 \\ 1 & MW < 30 \end{cases}$$

The correction factor (C) relative to CO for a product desorption spectrum is then

$$C = \frac{1}{F_m}\frac{1}{I_x}\sum_{\substack{\text{mass}\\ \text{fragment}}}\frac{F_m}{G_m \times T_m}$$

where the summation is over all mass fragments for the product species. The correction factors for the products from methanol on W(100)–(5 × 1)C are shown in Table A-2. The correction factor for hydrogen was obtained independently by comparing the desorption spectra for CO and H_2 for known coverages on W(100). Normalized desorption spectra were obtained by multi-

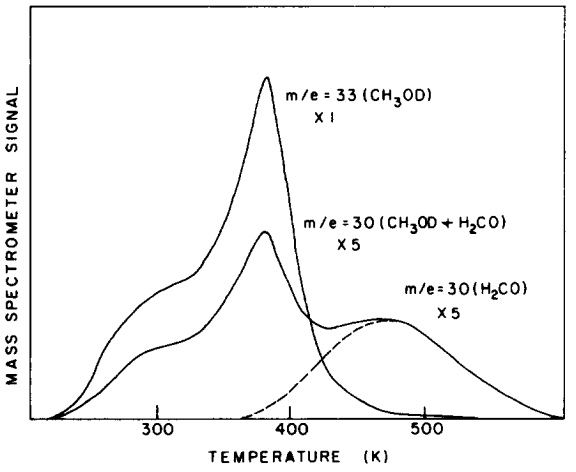

FIG. A-1. Correction of product desorption spectra for contributions of multiple products.

TABLE A-2

Normalization Correction Factors

Species	Mass fragment	Correction factor
CH_4	16	1.9
CO_2	44	1.4
CO	28	1
D_2	4	0.8
CH_3OD	33	2.3
CH_3OH	31	2.0
$HCOOCH_3$	60	5.9
H_2CO	30	2.5
H_2O	18	1.0

plying the product desorption spectrum by the correction factor. Normally it would be necessary to correct for differences in the pumping speed for different gases in the above correction factor. This problem was overcome by desorbing the products directly into the ionizer of the mass spectrometer so that fluxes were measured, rather than partial pressures.

Relative product yields were obtained by comparing the integrated areas under the corrected product desorption spectra. Absolute yields were obtained by comparing these yields with a known standard for CO(α) saturation on W(100)–(5 × 1)C, which was measured using standard pressure–temperature flash desorption techniques (*8*). The overall stoichiometry of the reaction products from formaldehyde, methanol-OD, and methyl formate were used as checks for the validity of the calculated product distributions (*9, 10*). In all cases the stoichiometry of the parent molecule was recovered on the W(100)–(5 × 1) surface. On the clean surface there was an overall hydrogen deficiency due to the displacement of hydrogen from the surface.

ACKNOWLEDGMENT

This work was supported by the NSF-MRL Program through the Center for Materials Research at Stanford University.

REFERENCES

1. Sinefelt, J. H., and Yates, J. D. C., *Nature Phys. Sci.* **229**, 27 (1971).
2. Levy, R., and Boudart, M., *Science* **181**, 547 (1973).
3. Ross, P. N., Jr., and Stonehart, P., *J. Catal.* **48**, 42 (1977).
4. Ross, P. N., Jr., and Stonehart, P., *J. Catal.* **39**, 298 (1975).
5. Ross, P. N., Jr., and Stonehart, P., *J. Electroanal. Chem.* **63**, 450 (1975).
6. McCarty, J., and Madix, R. J., *J. Catal.* **38**, 402 (1975).
7. Ko, E. I., and Madix, R. J., *Appl. Surface Sci.*, **3**, 236 (1979).
8. Benziger, J. B., Ko, E. I., and Madix, R. J., *J. Catal.* **54**, 414 (1978).
9. Benziger, J. B., Ko, E. I., and Madix, R. J., *J. Catal.*, in press.
10. Barteau, M. A., and Madix, R. J., *J. Catal.* **62**, 329 (1980).
11. (a) Worley, S. D., and Yates, J. T., Jr., *J. Catal.* **48**, 395 (1977); (b) "Eight Peak Index of Mass Spectra," 2nd ed., Vol. 1, p. 9, Mass Spectrometer Data Centre, Aldermaston, Reading, England, 1974.
12. Wachs, I. E., and Madix, R. J., *J. Catal.* **53**, 208 (1978).
13. Wachs, I. E. and Madix, R. J., *Surface Sci.* **76**, 531 (1978).
14. Housley, M., and King, D. A., *Surface Sci.* **32**, 479 (1972).
15. Benziger, J. B., Ko, E. I., and Madix, R. J., *J. Catal.* **58**, 149 (1979).
16. Falconer, J., and Madix, R. J., *J. Catal.* **48**, 262 (1977).
17. (a) Egelhoff, W. E., Perry, D. L., and Linnett, J. W., *J. Electron Spectrosc. Relat. Phenom.* **5**, 339 (1974); (b) Egelhoff, W. E., Linnett, J. W., and Perry, D. L., *Faraday Disc. Chem. Soc.* **60**, 127 (1975).
18. Foyt, D. C., and White, J. M., *J. Catal.* **47**, 260 (1977).
19. Matsushima, T., and White, J. M., *J. Catal.* **44**, 183 (1976).
20. Jesson, J. P., *in* "Transition Metal Hydrides" (El Muetterties, Ed.). Marcel Dekker, New York, 1971.
21. Bradley, D. C., *in* "Progress in Inorganic Chemistry," Vol. II, p. 303, Interscience Publishers, New York 1960.
22. Ko, E. I., and Madix, R. J., unpublished results.
23. Yates, J. T., Jr., and Madey, T. E., *J. Chem. Phys.* **54**, 4969 (1971).
24. Benziger, J. B., and Madix, R. J., *Surface Sci.* **75**, L379 (1978).
25. Gasser, R. P. H., Jackson, G. V., and Rolling, F. E., *Surface Sci.* **61**, 443 (1976).
26. UTI 100C Operating Manual (Uthe Technology International, Sunnyvale, CA, 1975).